J. Physiol. (1986), **370**, *pp.* 409–432
With 9 text-figures
Printed in Great Britain

THE ROLES OF PARACELLULAR AND TRANSCELLULAR PATHWAYS AND SUBMUCOSAL SPACE IN ISOTONIC WATER ABSORPTION BY RABBIT ILEUM

BY R. J. NAFTALIN AND S. TRIPATHI*
From the Department of Physiology, King's College, Strand, London WC2R 2LS

(*Received 14 June 1984*)

SUMMARY

1. Water movements have been studied in sheets of isolated rabbit ileum using a method which measures net volume flows across the mucosal and serosal surfaces of the tissue continuously with high resolution.

2. At 35 °C, with the tissues incubated in isotonic Ringer solution containing D-glucose (25 mM) on both sides, there is a steady net inflow of fluid at the rate of 24 ± 2 μl cm^{-2} h^{-1} across the mucosal surface (J_m) and an outflow of 8 ± 1 μl cm^{-2} h^{-1} across the serosal surface (J_s) ($n = 16$). The stable transepithelial p.d. across these tissues is $2{\cdot}7 \pm 0{\cdot}2$ mV, serosa positive. J_m can be reversibly inhibited by anoxia.

3. Ouabain (0·1 mM) added to the serosal solution inhibits inflow across the mucosal and serosal surfaces by 75% ($n = 7$) within 30 min.

4. If phlorizin (0·1 mM) is added to the mucosal Ringer solution containing glucose (20 mM) within 30 min of the commencement of *in vitro* absorption, J_m is reduced from 37 ± 3 to 28 ± 2 μl cm^{-2} h^{-1} ($n = 3$).

5. Dilution of the mucosal Ringer solution by 50 mosmol kg^{-1} (with the serosal solution kept isosmolar) results in a rapid transient increase in mucosal inflow. An increase of 50 mosmol kg^{-1} in the mucosal Ringer solution with NaCl, sucrose or mannitol causes a transient reversal of mucosal flow, followed by a return of inflow at a reduced level. Rabbit ileum can transport water against gradients of approximately 75 mosmol kg^{-1} of sucrose, NaCl, or mannitol.

6. Addition of polyethylene glycol (mol. wt. 20000; 3 mosmol kg^{-1}) causes a sustained reversal of mucosal inflow; inflow can be restored only by removing polyethylene glycol from the mucosal Ringer solution.

7. The tissue can absorb water against an osmotic gradient of 200 mM-glycerol.

8. The above data have been incorporated into a new model to explain isotonic flow of fluid by this epithelium. The main features are that the hydraulic conductivity (L_p) of the mucosal boundary of the lateral intercellular space is approximately 1×10^{-8} cm s^{-1} cmH_2O^{-1}. This L_p is too low to sustain isotonicity of the flow emerging from the lateral intercellular space at the observed rates. Hypertonic fluid emerging from the lateral intercellular space is diluted by transcellular water flow generated by the hypertonicity of the submucosa and back-diffusion of solute via mucosal shunt

* Present address: Department of Physiology, Yale University School of Medicine, New Haven, CT, U.S.A.

channels. The solute concentration of the submucosa at steady state is estimated to be only 2–5 % above the mucosal solution tonicity. Net absorption across the mucosa occurs simultaneously with a back-leak driven by the interstitial pressure into the mucosal solution via wide extracellular pores.

INTRODUCTION

The mechanism by which transepithelial transport of water is effected is as yet poorly understood. That water can be absorbed by epithelial systems against an apparent osmotic gradient was initially explained by the proposal that there were active transport mechanisms for translocating water (Parsons & Wingate, 1961). The demonstration that the paradoxical movement of water could be effected by an intraepithelial compartment which was hypertonic to the mucosal solution as a consequence of salt transport (Curran, 1960; Durbin, 1960; Curran & McIntosh, 1962) has been a viable alternative which has received much experimental support. There is little consensus, however, on the intraepithelial location(s) of the proposed hypertonic compartment and the osmotic gradients and hydraulic conductivities (L_p) necessary to achieve isotonic transport (see Weinstein & Stephenson, 1981). This is not surprising in view of the geometric constraints imposed by epithelia and the associated difficulty of measuring water movements with high time resolution. In a previous paper (Naftalin & Tripathi, 1985) a method was described which, to our knowledge, offers the highest resolution available for the continuous measurement of transepithelial water flow. This allows on-line measurement of water flow across both mucosal and serosal barriers of the tissue (which are usually unequal). With this new method it has become possible to study the dynamics of water flow produced by osmotic perturbations, instead of steady-state measurements of flow as has been done previously.

In this paper we show that the results of experiments carried out on actively transporting epithelium are consistent with the predictions of the passive hydraulic parameters determined previously in the non-transporting isolated rabbit ileum (Naftalin & Tripathi, 1985). Extracellular routes serve to permit both osmotic inflow of water from the intestinal lumen into the submucosa simultaneously with submucosal hydrostatic pressure-driven flows in the reverse direction. The transcellular flow is driven by the osmotic pressure gradient existing between the subcellular extracellular fluid and mucosal solution. A compartmental model simulating water and solute flows, which incorporates the observed L_p values of paracellular, transcellular, shunt and serosal routes shows that the submucosal solution is within 2–5 % of the tonicity of mucosal solution over a very wide range of osmolalities, despite the hypertonic fluid (15 % above the mucosal solution) emerging from the lateral intercellular space.

Preliminary accounts of this work have appeared (Naftalin & Tripathi, 1982 *a*, *b*, *c*, 1983).

METHODS

Adult New Zealand White rabbits of both sexes weighing 1·5–2·5 kg were rapidly killed with an overdose of sodium pentobarbitone (Sagatal, May & Baker) I.V. A segment of proximal ileum was removed and the lumen rinsed with warm (35 °C) oxygenated Ringer solution containing D-glucose

(25 mM); the highest rates of flow across the mucosal surface were observed in Ringer solution containing this concentration of D-glucose which was therefore used throughout the study. The peritoneum and longitudinal muscle layers were dissected away under warm Ringer solution and the tissue set up within 15 min in a chamber (Fig. 1, Naftalin & Tripathi, 1985) for measuring water flows.

Measurement of volume flows

The details of the method for measuring water flows have been described previously (Naftalin & Tripathi, 1985). Briefly, flow across the serosal surface (J_s) was measured by a capacitance transducer which detects changes in the height of the serosal solution. Flow across the mucosal surface (J_m) was determined by continuously measuring the rate of tissue volume change with an optical lever, and algebraically adding it to the serosal flow. Flow in the mucosa-to-serosa direction was considered as positive and flow in the reverse direction as negative.

Experiments described in the previous paper (Naftalin & Tripathi, 1985) were carried out at 20 °C and in the absence of D-glucose and HCO_3^- to prevent spontaneous flow. To elicit Na^+-pump-dependent net fluid transport, experiments in this series were carried out at $35 \pm 0{\cdot}01$ °C, this temperature being regulated by circulating water through a jacket surrounding the chambers (Haake, model E3). The mucosal solution was bubbled with humidified 95 % O_2–5 % CO_2 delivered down a glass capillary to a point just above the reflected light beam; oxygenation of the lower layers of the solution was facilitated by vigorous stirring with a magnetic stirrer bar. The agitation of the surface of the mucosal bathing solution produced by the breaking of small gas bubbles did not cause detectable tissue displacements if the hydrostatic head in the mucosal solution was > 3 cmH_2O above the serosal solution. The serosal solution was not oxygenated to permit measurement of flow across the serosal surface with the capacitance probe. Nevertheless the epithelium was sufficiently oxygenated from the mucosal side, as judged by its reversible sensitivity to anoxia (Fig. 2) and the absence of any pH change in the serosal bathing solution. The serosal solution was also stirred vigorously by magnetic stirring bars.

As expected, because of the stirring and raised temperature, the rate of evaporation from the serosal solution was higher (2 μl min^{-1}, or 12 μl cm^{-2} h^{-1} for 10 cm^2 of tissue) than at 20 °C, but was held constant by taking the precautions described earlier. The capacitance probe surface temperature was maintained at $30 \pm 0{\cdot}02$ °C with a heating element to prevent dew formation, which would interfere with the flow measurements. The final resolution of the optical lever was 2 μl cm^{-2} h^{-1}, which was less than that obtaining in the previous paper where the bathing solutions were at a lower temperature and were not bubbled.

Solutions and materials

Both surfaces of the tissue were bathed initially with a solution of the following composition (mM): D-glucose, 25; Na^+, 137; K^+, 4; Ca^{2+}, 1·2; Mg^{2+}, 1·2; Cl^-, 109·8; isethionate, 21·5; HCO_3^-, 10; HPO_4^-, 2; $H_2PO_4^-$, 0·5. Hypertonic solutions were prepared by the addition of the probe molecule to this basic solution, and hypotonic solutions by omitting sodium isethionate and variable amounts of NaCl. All reagents except the polyethylene glycol (mol. wt. 4000) were of analytical grade and were obtained from BDH or Sigma.

Electrical measurements

Transepithelial p.d. (V_{te}) was measured with 3 M-KCl–agar bridges and calomel half-cells connected to a millivoltmeter (Orion, model 701). Current bridges on the top and bottom of each hemichamber were made of Ringer solution–agar and were used to inject d.c. pulses from a constant-current source to monitor transepithelial resistance (R_{te}). One solution was earthed.

Analysis of data

Data, except with ouabain, were included in the study only if the effects were reversible and bracketed by two control periods. Each number represents one observation period on one animal. Variability of the data was expressed as the mean $\pm$S.E. of mean. Tests of significance were made using Student's t test.

A compartmental model simulating isotonic transport across rabbit ileum

Because of the complexity of the network of routes across the tissue, it was necessary to use a computer model combining the elements described to model the transient and steady-state flows which occur following perturbations of solution osmolality. This provides a framework for description of a near-isotonic fluid transport system. (Fig. 1).

Simulation of fluid and solute movement across three parallel pores within the mucosal surface, a distensible submucosa and a serosal surface with a single pore size was carried out by numerical solution of a series of simultaneous differential equations, using fourth-order Runge–Kutta methods. The details of the equations for flow of solutes and water are described in the Appendix.

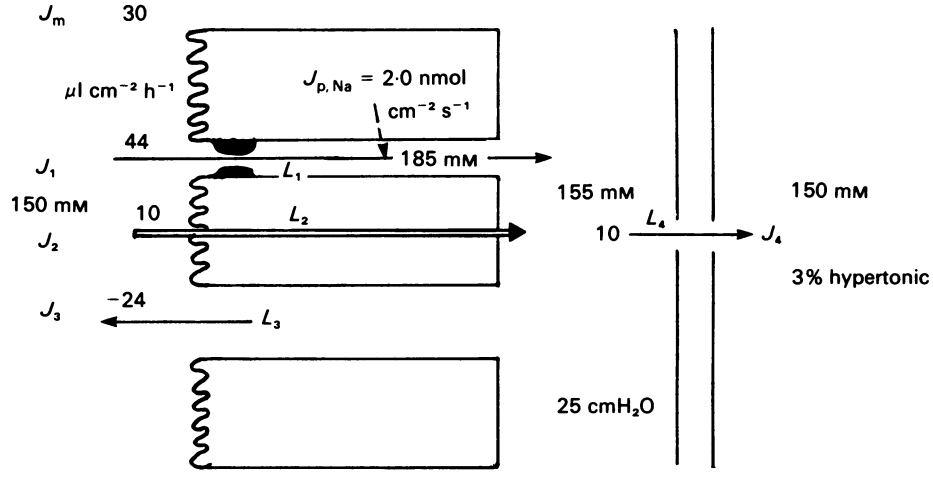

Fig. 1. Diagram showing the routes of fluid movement across the mucosal and serosal surfaces of the intestine with estimates of the local concentrations of NaCl and flows at steady state. $J_{p,Na}$ is Na^+-pump driven Na^+ flux.

RESULTS

Tissues which were incubated with isotonic Ringer solution containing D-glucose (25 mM) on both sides had initial absorption rates across the mucosal surface (J_m) of 24 ± 2 μl cm^{-2} h^{-1}, and across the serosal surface (J_s) of 8 ± 1 μl cm^{-2} h^{-1} ($n = 16$). The average stable electrical p.d. in these tissues was $2{\cdot}7 \pm 0{\cdot}2$ mV, serosa positive. The p.d.s were approximately twice this average value when the tissues were initially set up, and declined over a period of approximately 20 min to their stable values. However, no significant correlation between p.d. and J_m was detectable. Resistance measurements were not made continuously to prevent possible electro-osmotic effects, but in a small sample were found to average 85 ± 7 Ω cm^2 ($n = 6$). All flows reported here were obtained under open-circuit conditions. Flows and p.d.s were stable for 4–5 h, although the rates of tissue expansion slowed down progressively with filling of the submucosa.

Effects of inhibitors on water flows

Anoxia. J_m and p.d. were reversibly inhibited by substituting N_2 for O_2 in the mucosal Ringer solution ($n = 3$; Fig. 2). Inflow across the mucosal surface fell with a half-time of approximately 5 min after switching to N_2. The flow across the serosal

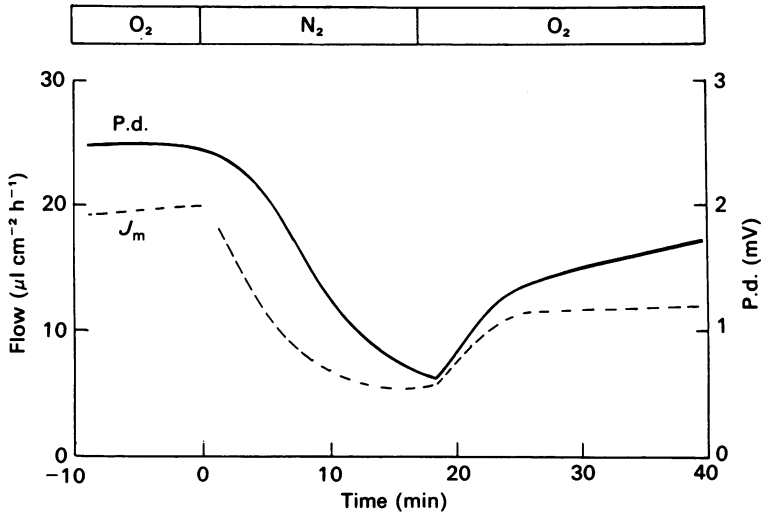

Fig. 2. Flow across the mucosal surface, J_m, and transepithelial p.d. (V_{te}) are plotted on the ordinate as a function of time ($n = 3$).

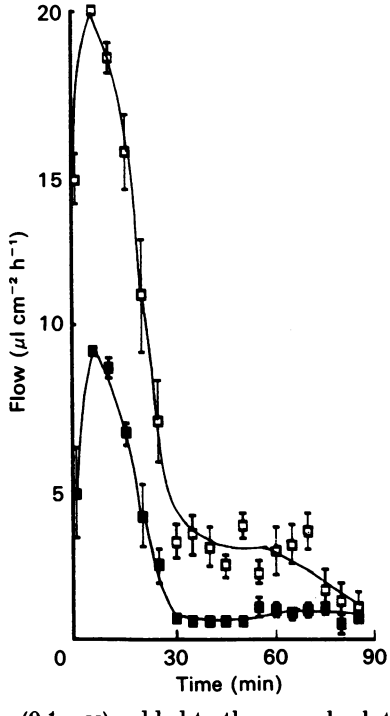

Fig. 3. Effect of ouabain (0·1 mM), added to the serosal solution at time zero on flow, J_m (□) and J_s (■); error bars are S.E. of mean ($n = 7$).

surface (not shown) was unaffected by anoxia. Following return of O_2 there was a rapid recovery of inflow; however, the extent of recovery was variable and depended on the duration of anoxia.

Ouabain. Ouabain (0·1 mM), added to the serosal solution, induced a rapid initial increase in both J_m and J_s (Fig. 3). J_m increased from $14·6 \pm 0·8$ to $19·8 \pm 0·43$ μl cm^{-2} h^{-1} within 5 min ($P < 0·01$); J_s increased from $4·6 \pm 1·4$ to $9·1 \pm 0·35$ ($n = 7$) μl cm^{-2} h^{-1} within 5 min ($P < 0·01$). Thereafter, J_m decreased from 20 ± 1 to $3 \pm 0·5$ μl cm^{-2} h^{-1} within 30 min ($n = 7$) and the p.d. from $3·0 \pm 0·6$ to $0·5 \pm 0·3$ mV; J_s decreased from $9 \pm 0·4$ to $0·5 \pm 0·2$ μl cm^{-2} h^{-1} during the same time. The effects of ouabain were not reversible. Residual J_m and J_s remained for periods exceeding 90 min and were unaffected by raising the concentration of ouabain to 0·5 mM ($n = 3$) (not shown) had no significant effect. However, on increasing the concentration of D-glucose in the mucosal Ringer solution to 50 mM, the residual mucosal flow J_m decreased, initially to a net outflow and then permanently to zero ($n = 3$; results not shown); this result differs from the effect of raising the D-glucose concentration to 50 mM with control tissue untreated with ouabain, when full recovery of inflow was observed.

Effects of addition of D-glucose on water flows

Following an initial 15–20 min period of incubation in glucose-free Ringer solution, D-glucose (20 mM) was added to both mucosal and serosal sides, and a rapid increase in mucosal inflow was observed without any concurrent increase across the serosal surface (Fig. 4*A*). The time course of increase shows that the stimulation was maximal 20–30 min after exposure to D-glucose ($10 \pm 2·2$ μl cm^{-2} h^{-1} from an initial rate of 1–2 μl cm^{-2} h^{-1}) ($n = 5$). Electrical transepithelial p.d. also increases simultaneously with the rise in mucosal inflow, from 0 to 5 mV.

Effects of substitution of D-glucose on J_m and p.d.

Following incubation for 1 h in Ringer solution containing 25 mM-D-glucose, the D-glucose in the mucosal Ringer solution was substituted isosmotically for 10 min periods with mannitol ($n = 3$), α-methyl-D-glucoside ($n = 2$), or 3-*O*-methyl-D-glucose ($n = 2$). In none of these tissues was flow significantly reduced ($P > 0·5$). There was a small reversible reduction in p.d. with mannitol substitution ($0·3 \pm 0·1$ mV, $P < 0·05$), but not when replacement was with the other sugars ($P > 0·05$; Fig. 4*B*).

Effects of phlorizin on J_m

If phlorizin (0·5 mM) was added to the mucosal solution after a prolonged incubation of > 1 h, it was without significant effect on J_m ($n = 6$). However, when phlorizin (0·1 mM) was added after only a short incubation period (10–15 min) J_m decreased from 37 ± 3 to 28 ± 2 μl cm^{-2} h^{-1} ($n = 3$; $P < 0·01$; Fig. 4*C*) within 2–4 min, and the p.d. decreased from 2·5 to 1·5 mV. This effect was reversed after phlorizin was removed. The findings in Fig. 4 indicate that the glucose concentration of the mucosal bathing solution ceases to affect inflow across the mucosal surface after the tissue has been exposed for a period of 1 h.

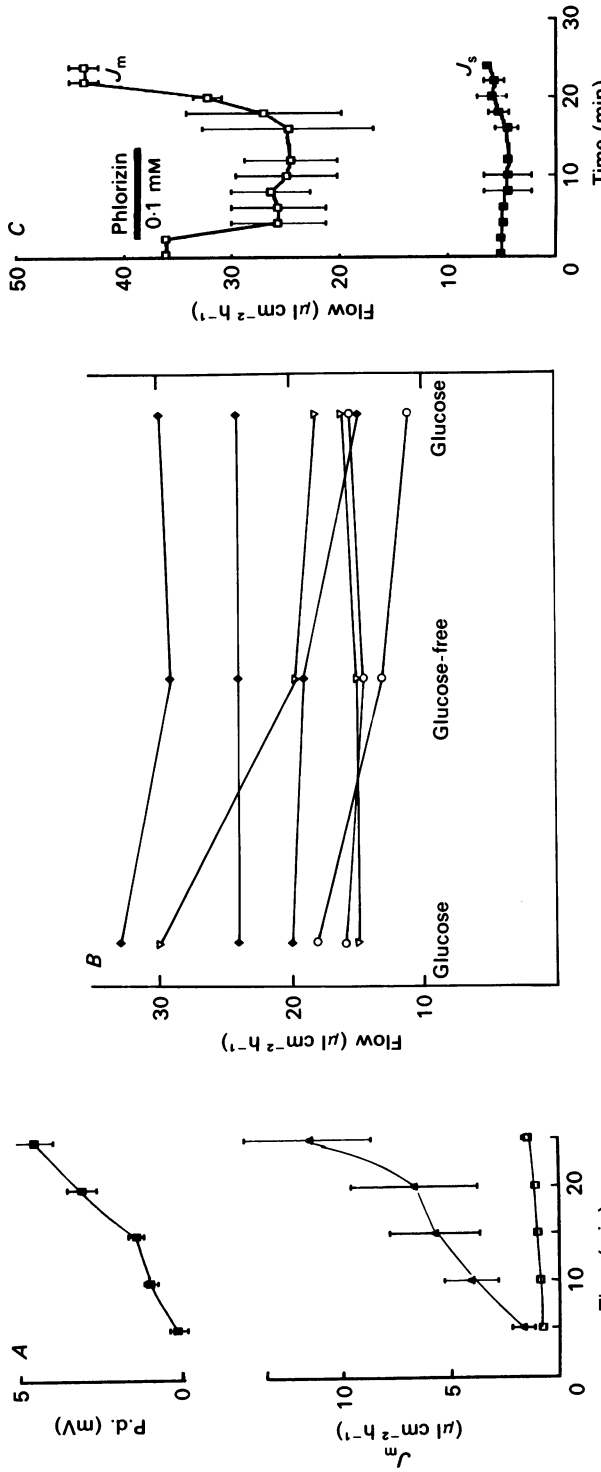

Fig. 4. *A*, effect of D-glucose (20 mM) to the mucosal and serosal solution on p.d.; J_m and J_s ($n = 7$). *B*, isosmotic replacement of 25 mosmol D-glucose kg^{-1} with D-mannitol (◆), 3-*O*-methyl-D-glucose (▽), α-methyl-D-glucoside (○) following a period of approximately 1 h sustained absorption. *C*, the effect of addition of phlorizin (0·1 mM) to the mucosal solution on J_m (□) and J_s (■) at 2 min and removal of phlorizin by replacement of the mucosal solution with fresh glucose Ringer solution at 14 min. Error bars are S.E. of mean of three experiments. The data are normalized to flows measured immediately prior to addition of phlorizin.

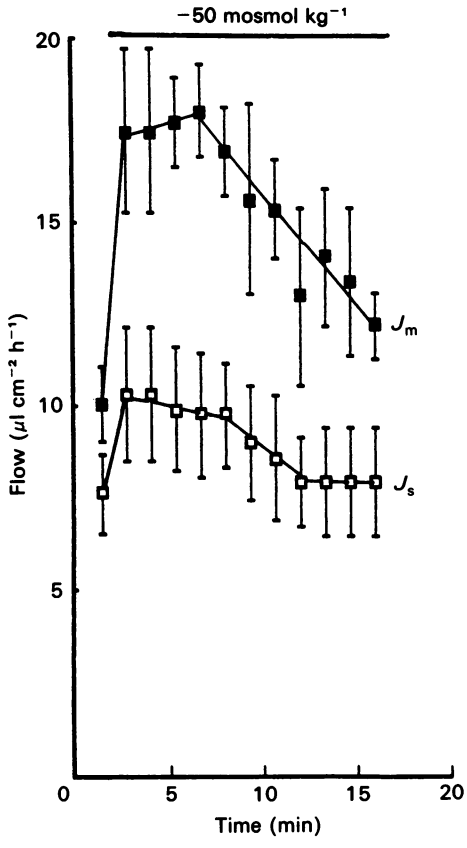

Fig. 5. Effect of dilution of the mucosal bathing solution by 50 mosmol kg^{-1} by removal of isethionate on uptake across the mucosal surface, J_m (■) and across the serosal surface, J_s (□) ($n = 6$). The solution was made hypotonic at the beginning of the bar.

Effects of changing tonicity of the mucosal solution on water flows across the mucosal and serosal surfaces

(*1*) *Effects of mucosal dilution.* When the mucosal solution was diluted by 50 mosmol kg^{-1}, the average inflow across the mucosal surface, J_m, increased rapidly from $10 \pm 1{\cdot}2$ to above $17 \pm 2{\cdot}4$ μl cm^{-2} h^{-1} ($P < 0{\cdot}001$) and the average J_s from $7 \pm 1{\cdot}4$ to $10 \pm 1{\cdot}7$ μl cm^{-2} h^{-1} ($n = 6$; $P < 0{\cdot}01$ (paired t-test); Fig. 5). This rapid increase in J_m occurred within the first 30 s of exposure to hypotonic solution. After 5 min, the mucosal inflow began to decrease steadily and significantly (t test of slope $P < 0{\cdot}001$). The observed p.d. values fell after dilution due to the Na^+ diffusion potential across the mucosal surface.

(*2*) *Effects of mucosal hypertonicity.* Increasing the mucosal tonicity to different extents had the following effects.

(a) Increasing the tonicity of the mucosal bathing solution by 50 mosmol NaCl kg^{-1} had a biphasic effect on J_m. After a control period during which inflow across the mucosal surface was 29 ± 3 μl cm^{-2} h^{-1}, addition of NaCl to the mucosal

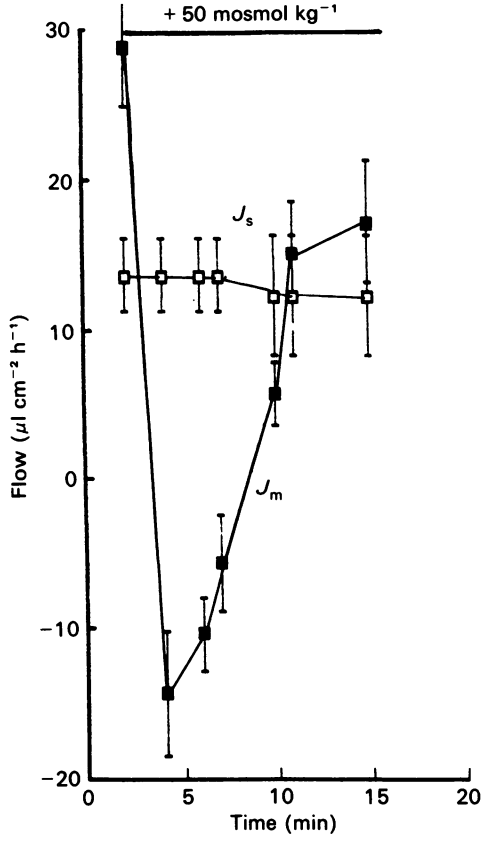

Fig. 6. Effect of raising the mucosal tonicity by 50 mosmol kg^{-1} with NaCl ($n = 7$) on mucosal inflow, J_m (■) and serosal outflow, J_s (□). Negative J_m signifies mucosal outflow.

solution induced an immediate reversal of flow so that the direction of net flow reversed to an outward flow of 14 ± 4 μl cm^{-2} h^{-1} (Fig. 6). The initial change in rate was too rapid to follow accurately with the methods employed; however, it can be seen that half-time was less than 20 s. After 2 min, the outflow began to decrease and reached zero net flow within 5–9 min following exposure to the hypertonic solution. Mucosal inflow reached a new steady rate of 17 ± 3 μl cm^{-2} h^{-1} ($n = 7$) after 10–14 min (Fig. 6). During this time outflow across the serosal border gradually decreased from 13 ± 2 to 11 ± 2 μl cm^{-2} h^{-1} ($P < 0{\cdot}05$, paired t test).

The same pattern of flow change was also observed when the mucosal solution was made hypertonic with mannitol (50 mM) and with sucrose (50 mM) ($n = 7$). After addition of NaCl (25 mM), the p.d. first increased by $0{\cdot}4 \pm 0{\cdot}2$ mV and then decreased to control levels. The rise in p.d. was probably due to the Na^+ diffusion potential, and the subsequent fall was possibly due to solute equilibration within the submucosal solution. The biphasic response of p.d. after tonicity change was not seen when non-electrolytes were added to the mucosal solution, when the average reduction in p.d. was 1 mV.

(b) A step increase of 100 mosmol kg^{-1} in the mucosal tonicity was made using

non-electrolytes (mannitol, sucrose and polyethylene glycol (mol. wt. 400). J_m reversed from an inflow in control conditions to a rapid outflow. Following the rapid initial outflow a slower outflow rate, close to zero, was observed (Fig. 7). Only on returning to isotonic Ringer solution in the mucosal solution was it possible to restore positive net inflow. In these experiments the p.d. decreased by 2·7 mV ± 0·7 mV ($n = 3$).

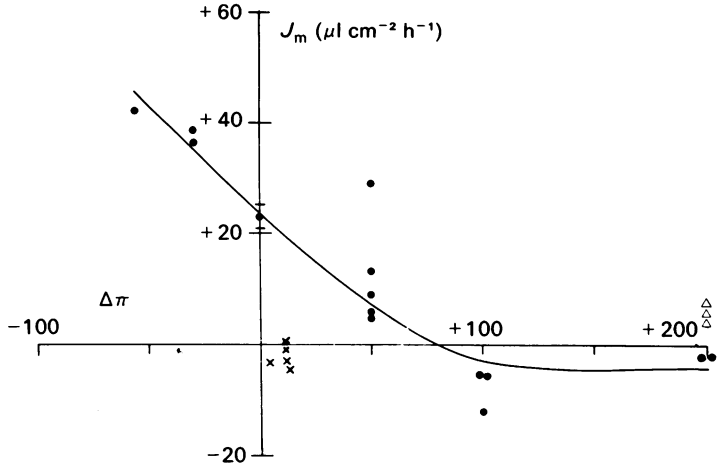

Fig. 7. The effects of changing the tonicity of the mucosal solution, with the serosal solution kept isosmotic, on J_m. J_m in μl cm^{-2} h^{-1} is plotted on the ordinate as a function of mucosal osmolality (mosmol kg^{-1}). The ordinate is the isosmotic line, with dilution of the mucosal Ringer solution shown on the negative abscissa and mucosal hypertonicity shown on the positive abscissa. The positive ordinate represents mucosal–serosal flow. Control values ± S.E. of mean are grouped on the ordinate. ●, alterations of J_m generated by NaCl, sucrose, mannitol, polyethylene glycol (mol. wt. 400). The epithelium can absorb water against gradients of up to 75 mosmol kg^{-1} of these molecules. However, 5–12·5 mosmol kg^{-1} of polyethylene glycol (mol. wt. 4000) (×) abolishes inflow. In contrast, absorption still continues against 200 mosmol of glycerol (△). The non-linearity of the line (fitted by eye) is due to collapse of the submucosal space with hypertonic solutions.

(c) A step increase of 200 mosmol NaCl kg^{-1} abolished inflow reversibly, with a rapid initial outflow falling to zero flow (Fig. 7). The p.d. first increased by an average of 0·4 mV and then declined by 1·8 mV ($n = 2$).

Net flows: to determine the limit of the hypertonicity against which net absorption can be maintained and to determine the time course of the flow changes following step changes in the tonicity of the mucosal solution, the composition of the mucosal solution was altered, with the serosal solution kept at a fixed concentration. Fig. 7 illustrates the results of twenty-one experiments in which the mucosal solution was either diluted or made hypertonic. The maximal changes in inflow J_m measured at the turning point, with respect to control values observed in isotonic solution, are plotted as a function of tonicity change. It can be seen that for positive values of J_m there was a fairly linear relationship between the mucosal tonicity change and mucosal inflow. Zero inflow can be seen to occur when the mucosal tonicity was increased by 75 mosmol kg^{-1}. The linear response to tonicity did not extend into the domain where steady-state net outflow occurs.

This asymmetry of force–flow relationship determining mucosal water flow has been discussed previously (Naftalin & Tripathi, 1985) and it results from a change in interstitial pressure from positive to negative values when steady-state mucosal net inflow changes to outflow.

Large deviations from the relationship between mucosal tonicity and flow can be seen in Fig. 7 with polyethylene glycols (mol. wt. 4000 and 6000) (×) and with glycerol (△). The data with polyethylene glycol (mol. wt. 20000) were not included in Fig. 7 (see below).

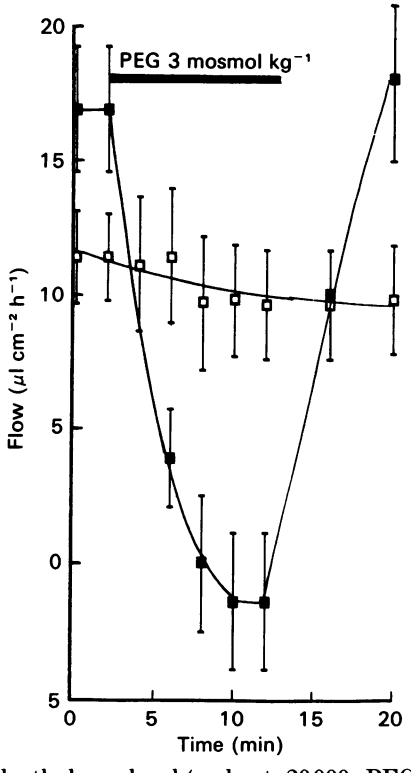

Fig. 8. Addition of polyethylene glycol (mol. wt. 20000; PEG; 3 mosmol kg^{-1}) ($n = 3$) to the mucosal solution at 2 min leads to a sustained reduction in J_m (■) without significant effect on J_s (□). Removal of PEG at 14 min restores J_m.

(*3*) *Effects of macromolecules.* The flow patterns observed with low concentrations of high molecular weight solute and high concentrations of low molecular weight solutes were strikingly different. The effect of polyethylene glycol (mol. wt. 20000; 3 mosmol kg^{-1}) (corrected for osmotic activity using a Wescor vapour pressure osmometer) added to the mucosal solution on J_m and J_s are shown in Fig. 8. Following addition of the macromolecule, J_m decreases to zero or to negative values. There was no recovery of inflow until after the polyethylene glycol was removed from the mucosal solution. Flow across the serosal surface was relatively unaffected by this perturbation across the mucosal surface. Despite the large changes in flow, the p.d.

was only reduced by 0·06 mV. On the other hand, addition of glycerol (200 mM) to the mucosal solution caused only a transient reversal of flow which rapidly reverted to a positive net inflow ($n = 3$; Fig. 7). The p.d. was reduced by an average of 20 mV which was a 5-fold greater change per osmole than observed with polyethylene glycol.

DISCUSSION

The effects of changing the tonicity of the mucosal bathing solution

Changing the tonicity of the mucosal solution produced several different tissue responses.

First, dilution of the mucosal solution (Fig. 5) results in a rapid increase in mucosal inflow. This is followed by a slow decline. The decrease in mucosal inflow is not accompanied by a concurrent change in outflow across the serosal surface, indicating that the change is not due to a change in interstitial pressure.

Secondly, raising the tonicity of the mucosal solution with NaCl or sucrose causes a rapid decrease of inflow across the mucosal border, followed by a slower recovery phase, the extent of recovery being dependent on the step size of the tonicity increase (Fig. 7).

Thirdly, a small rise in the tonicity of the mucosal solution due to addition of polyethylene glycol (mol. wt. 20000) (Fig. 8) induces a rapid and large decrease in inflow. If the change in flow is calculated per osmole of hypertonicity it can be seen that polyethylene glycol is 10–20-fold more effective than NaCl in inhibiting J_m. There is no recovery in inflow following addition of polyethylene glycol until it is removed from the mucosal solution (Fig. 8). This contrasts with the rapid rebound in flow seen with hypertonic NaCl or sucrose (Fig. 6). The large decrease in fluid inflow induced by polyethylene glycol (mol. wt. 20000) is accompanied only by a negligible change in V_{te}, whereas hypertonic sucrose or NaCl have large effects on V_{te}. When expressed on an osmolal basis the change in p.d. is 5–10-fold greater with NaCl than with polyethylene glycol.

Fourthly, glycerol (200 mM) added to the mucosal solution has only a small effect on mucosal inflow but exerts a maintained effect on streaming potential (Fig. 7).

The importance of the wide shunt pathway between the submucosa and mucosal solution

Evidence for a wide shunt across the mucosal surface of rabbit ileum has been presented previously (Naftalin & Tripathi, 1985). The results presented in this paper, namely the high osmotic flow induced by macromolecules with low streaming potentials, confirm those reported previously. As the change in J_m induced by macromolecules is much larger than would be predicted if flow is via a single set of channels having a significant reflexion coefficient for NaCl and sucrose, the existence of separate wide shunt channels of high L_p is required to explain these data. Channels with an L_p of approximately $1{\cdot}5 \times 10^{-7}$ cm s^{-1} cmH_2O^{-1} in parallel with channels which have a reflexion coefficient for NaCl and sucrose close to 1 and a low L_p (*ca.* 1×10^{-8} cm s^{-1} cmH_2O^{-1} are consistent with the data.

The absence of any return of mucosal outflow towards the resting level following

addition of macromolecules (Fig. 8), in contrast to the reversal of outflow observed when the mucosal solution is raised with NaCl or sucrose (Fig. 6), shows that the shunt pathway permits diffusion of low molecular weight, but not of high molecular weight solutes between the mucosal bathing solution and submucosa. Equilibration of osmotic solute between the mucosal solution and submucosa reduces the transmucosal osmotic gradient, and hence the mucosal outflow.

The slow rise in submucosal tonicity following an increase in concentration of the mucosal solution indicates: (a) that the solute tonicity within the submucosal compartment can differ from that in either the serosal bathing solution or the lateral intercellular space; (b) that there is a relatively slow rate of solute equilibration between the submucosa and serosal solution; if solute equilibration between the submucosa and serosal solution were rapid, no significant rise in submucosal concentration could occur on raising the mucosal solute concentration; (c) the solute concentration within the submucosa is not controlled solely by the Na^+-pump activity of the mucosa and/or unstirred layer effects, as suggested by Diamond (1979) and Barry & Diamond (1984); if this were true, then recovery of inflow after a step increase in mucosal tonicity should be the same whether NaCl, sucrose or macromolecular solute is added to the mucosal solution. The rebound rise in inflow after raising the mucosal NaCl tonicity and the absence of rebound when macromolecules are added demonstrates that the rebound recovery phase is due to low molecular weight solute equilibration across the wide shunt pathway between the mucosal and submucosal solutions and not to concentration polarization.

The unstirred layer effect

The half-time for the decrease in J_m induced by polyethylene glycol (mol. wt. 20000) is 30–45 s (Fig. 8). The half-time for the decrease induced by NaCl is approximately 10 s (Fig. 6).

It is possible to estimate the unstirred layer thickness from the half-time of the osmotic flow transient, $t_{\frac{1}{2}}$ as follows (Diamond, 1966; Barry & Diamond, 1984):

$$l = \sqrt{(t_{\frac{1}{2}} . D/0{\cdot}38)},$$

where l is the unstirred layer thickness and D the diffusion coefficient of the osmotic probe.

The diffusion coefficient of polyethylene glycol (mol. wt. 20000) in aqueous solution is approximately 5×10^{-7} cm^2 s^{-1} and of sucrose is approximately 4×10^{-6} cm^2 s^{-1} (Schultz & Solomon, 1961; Renkin, 1973). Thus for polyethylene glycol, the external unstirred layer thickness is approximately 50–100 μm and for sucrose and NaCl also approximately 100 μm. The half-time measurement for polyethylene glycol is more accurate than for NaCl.

The 'sweeping away' effect resulting in a reduced surface concentration of the osmotic probe can be estimated to a first approximation from the following relationship (Wright, Smulders & Tormey, 1972):

$$C_0 = C_1 \exp \frac{(-J_v . l)}{D},$$

where C_0 is the surface concentration, C_1 the solution concentration, J_v the osmotically induced flow, l the unstirred layer thickness and D the diffusion coefficient of the osmotic probe.

$$C_0/C_1 > 0{\cdot}95,$$

where J_v is 20 μl cm^{-2} h^{-1}, $l = 50$ μm and $D = 5 \times 10^{-7}$ cm^2 s^{-1}.

Thus the 'sweeping away' effect external to the mucosal surface is negligible. Hence any difference between the L_p values measured with NaCl, sucrose and polyethylene glycol cannot be due to a difference in the unstirred layer effects external to the mucosa.

Concentration polarization in the lateral intercellular space and estimation of the L_p of the transcellular route

Osmotic flow induced by a NaCl gradient can only take place across those channels which have a finite reflexion coefficient for NaCl. It follows that active fluid absorption cannot be generated by the action of the Na^+ pump within the wide shunt channels. Hence, the appropriate L_p to generate the osmotic gradient required for fluid absorption is that of the channels which reflect NaCl. Diamond (1979) has argued that the real L_p of this route in rabbit gall-bladder is very high, but is apparently low because solute polarization within the lateral intercellular space reduces the osmotic pressure gradient across the mucosa. This argument can be refuted, for rabbit small intestine at least, by the results presented here and in the previous paper (Naftalin & Tripathi, 1985). If hydraulic flow across the intestine is via a single class of channel having a high L_p (1×10^{-7} cm s^{-1} cmH_2O^{-1}), then the osmotic flow induced across this pathway by oncotic pressure e.g. with polyethylene glycol 20000 should be substantial and solute polarization would result in a retardation of outflow, as seen with hypertonic NaCl in the mucosa. Furthermore, addition of 1·25 mM-NaCl to the mucosal solution tonicity should have approximately 50 % of the effect observed with polyethylene glycol (mol. wt. 20000) at 3 mosmol kg^{-1}. As neither of these effects is observed, this indicates that the L_p of the transcellular route is substantially below that of the wide shunt pathway, i.e. approximately 1×10^{-8} cm s^{-1} cmH_2O^{-1}.

The role of the submucosa in producing quasi-isotonic absorbates

There has been a prolonged debate concerning the role of the lateral intercellular space in producing isotonic absorbates. Hill (1975, 1980) and Sackin & Boulpaep (1975) drew attention to the shortcomings of the Diamond & Bossert (1967) model of quasi-isotonic absorption, showing that the L_p of the lateral intercellular space boundaries would have to be very high to support a quasi-isotonic absorbate. The rejoinder (Diamond, 1979; Barry & Diamond, 1984) that unstirred layer effects mask the high mucosal L_p is not supported by the experimental results and analysis in this paper, which show that the unstirred layer effect external to rabbit ileal mucosa is insubstantial. However, because the volume of the lateral intercellular space is small (20–25 μl cm^{-2} serosal area), and the rate of solute pumping is rapid (1–2 nmol s^{-1} cm^{-2} serosal area), a step change in the tonicity of the mucosal solution is followed by a rapid adjustment in the tonicity of the lateral intercellular space, so that transient change in flow into the lateral intercellular space, even with

the relatively low L_p (1×10^{-8} cm s^{-1} cmH_2O^{-1}), is complete within a few seconds. This means that Diamond's (1979) view that the unstirred layer effects can nullify the effect of a step change in external tonicity on osmotic flow into the lateral intercellular space, so that the L_p of the lateral intercellular space boundary is indeterminate, is correct.

However, the large amplitude and prolonged duration of the flow transients actually observed following step changes in mucosal solution tonicity (Figs. 5, 6 and 8) indicate that osmotic flow is not determined solely by solute and water movements between the lateral intercellular space and mucosal solution, but must also involve some larger compartment which can equilibrate slowly towards the mucosal solution tonicity. Simulation of a submucosal fluid tonicity close to that of the mucosal solution requires only that there should be (a) a low transcellular L_p (1×10^{-8} cm^{-2} s^{-1} cmH_2O^{-1}), permitting solute-free fluid movement between the mucosal and submucosal solutions generated by the osmotic pressure difference between the submucosal compartment and mucosal bathing solution, and (b) a pathway permitting equilibration of low molecular weight solutes between the mucosal and submucosal compartments, namely the wide mucosal shunt pathway.

The transcellular route of water movement need not be confined to those few cells which are engaged in salt export; transcellular flow via quiescent cells in inactive tissue regions also serves. Thus, despite the fact that the area of basolateral membranes is 10–20-fold greater than the area of membrane facing the submucosa (Blom & Helander, 1977), the L_p of the transcellular route, expressed in terms of serosal area, will be of same order of magnitude as that of mucosal–basolateral route. Thus water flow across the transcellular route is an important determinant of over-all transmucosal water flow and will be the dominant factor determining the transient changes in flow following a step change in tonicity of the mucosal bathing solution. This arises because the transient change in tonicity within the lateral intercellular space will be rapid, but the osmotic pressure difference between the submucosa and mucosal solution will adjust more slowly, because the submucosal space volume is both larger and more distensible than the lateral intercellular space and there is little direct salt pumping into the submucosal space.

The wide shunt pathway permits passage of low molecular weight solutes. Thus, as well as increasing the rate of solute equilibration between the mucosa and submucosa, the presence of the shunt pathway prevents concentration polarization and 'sweeping away' effects within the submucosa, as predicted by Diamond (1979), because the salt gradients will be dissipated via the shunts. This means that the measured L_p of the transcellular route can be considered to be an accurate estimate of the true value.

Recent estimates of the L_p of rabbit brush-border membrane vesicles (Van Heeswijk & Van Os, 1984) indicate that the permeability of these membranes is approximately the same as that observed here for transcellular flow. The model presented here shows that a near-isotonic submucosal compartment can coexist with lateral intercellular spaces which may have substantial hypertonicity. Such large tonicities have been observed previously using electron microprobe techniques in rabbit ileum transporting D-galactose (Gupta, Hall & Naftalin, 1978). Thus it is seen that the submucosal compartment, by permitting osmotic equilibration of water

across the transcellular route and salt equilibration via the shunt channels, determines the net flows across the mucosa and the tonicity of fluid leaving the tissue across the serosal surface.

Analysis and simulation of osmotic flow transients across rabbit intestine

An alternative to the steady-state approach to estimating the L_p of the transmucosal route is to analyse the transient response to tonicity change within the mucosal solution. A sudden increase in concentration of NaCl in the mucosal solution will reduce or reverse the direction of the osmotic pressure gradients existing between both the lateral intercellular and submucosal spaces and mucosal solution. This leads to a reduction or reversal of flow between the mucosal solution and lateral intercellular space via the tight-junction and transcellular routes. The initial rate of reduction of inflow depends on (a) the unstirred layer effect at the external surface of the mucosa and (b) the small volume of the lateral intercellular space.

Because water inflow to the lateral intercellular space is slowed by a rise in the external osmotic pressure, the concentration of solutes within the lateral intercellular space will rise because of (i) continued solute pumping and (ii) concentration polarization of solute within the lateral intercellular spaces. As the solute concentration within the lateral intercellular space increases, the rate of fluid inflow will recover. The recovery rate of mucosal fluid inflow, J_1 (Fig. 1) depends on (a) the L_p of the routes between the mucosal solution and lateral intercellular space (the transcellular and tight-junctional routes combined), (b) the volume of the lateral intercellular space, and (c) the Na^+-pump rate. The higher the L_p, the smaller the lateral intercellular space volume and the faster the pump rate, the faster will be the rate of recovery of mucosal inflow.

In practice the very small volume of the lateral intercellular spaces (20–25 μl cm^{-2} serosal area), combined with the observed rate of solute pumping (0·5–2 nmol s^{-1}) and L_p of the tight junction and lateral membranes $\approx 1\text{–}2 \times 10^{-8}$ cm s^{-1} cmH_2O^{-1} mean that recovery of inflow into the lateral intercellular space following osmotic perturbation in the mucosal solution is so rapid that it cannot account for the slow changes in J_m which are observed following osmotic perturbations (Figs. 5 and 6).

Submucosal space. In addition to the changes in flow between the mucosal solution and lateral intercellular space, a step change in mucosal solution tonicity will also cause a change in transcellular flow between submucosa and mucosal solution. This response will also return towards control rates as the solute concentration within the submucosa equilibrates with the altered mucosal concentration. This rate of recovery depends on the L_p of the transcellular route, the size of the submucosal compartment and the rate of solute permeation between submucosa and mucosal solutions via the shunt pathway. Simulation of the transient changes in flows across the mucosal and serosal surfaces following a step increase or decrease (see Appendix) of 50 mosmol kg^{-1} in the bulk mucosal solution, and an unstirred layer effect with half-time = 13·8 s, shows that the observed flows (Fig. 6) are consistent with an L_p of the tight-junctional route of approximately 7×10^{-9} cm s^{-1} cmH_2O^{-1} and for the transcellular route an L_p of 5×10^{-9} cm s^{-1} cmH_2O^{-1}. At least 50 mosmol kg^{-1} osmotic pressure difference (*ca.* 25 mM-NaCl) is required to generate water flows at a rate of 20–50 μl cm^{-2} h^{-1}

between the lateral intercellular space and the mucosal solution, when the L_p of this route is 1×10^{-8} cm s^{-1} cmH_2O^{-1}. This is the range of concentration differences observed in lateral intercellular space of rabbit ileum with electron microprobe microanalysis (Gupta *et al.* 1978). With the bathing solution osmolality clamped at 300 mosmol kg^{-1} (150 mM) the predicted steady-state salt concentration within the submucosa is 155 mM. An interstitial pressure of 20–30 cmH_2O is sufficient to drive flow across the serosal surface with a serosal surface L_p of 7×10^{-8} cm s^{-1} cmH_2O^{-1} at rates within the observed range of 10–15 μl cm^{-2} h^{-1}.

Influence of the submucosal tonicity on transmucosal water flow

(*1*) *Effects of* D*-glucose.* Smyth & Taylor (1957) observed that hydraulic-pressure-induced flow across rat intestine was increased in the presence of D-glucose. They deduced that the presence of D-glucose raised interstitial pressure and thereby increased the hydrostatic-pressure-induced flow.

Accumulation of D-glucose will also increase the submucosal tonicity, which will increase transcellular flow and raise the interstitial pressure. The time-dependent increase in inflow across the mucosal surface (Fig. 4*A*) reflects this accumulation of D-glucose within the submucosa, and the increase in serosal exit will reflect the raised interstitial pressure.

If phlorizin is added to the mucosal solution following only a brief exposure to D-glucose, then a rapid fall in fluid inflow is observed; this finding is consistent with a close correlation between Na^+ and glucose movement, as has been well established (for review see Crane, 1977). However, if the tissue is exposed to D-glucose for 1 h, no significant effect on J_m is observed (Fig. 4*B*) by substituting either mannitol, 3-*O*-methyl-glucose or α-methyl glucoside. These results suggest that when the submucosa becomes loaded with sugars, J_m becomes independent of coupled Na^+–glucose movement across the apical border of glucose-transporting cells because the osmotic effect of the accumulated sugars within the submucosa sustains mucosal inflow during the period when the sugar is absent from the mucosal solution.

(*2*) *Effect of ouabain on transmucosal water movements.* Further evidence of effects of submucosal solutes on mucosal inflow comes from the sustained mucosal fluid inflow following exposure of the tissue to high concentrations of ouabain (Fig. 3). During the first period of inhibition, when the Na^+ pump is inhibited, J_m declines rapidly. This inhibition of the Na^+ pump will reduce the tonicity of NaCl within the lateral intercellular space to the same level as is present within the submucosa. However, a small net residual fluid inflow across the mucosal surface is still observed for prolonged periods of 1–2 h. This sustained inflow is consistent with osmotic-pressure-driven flow from a large, slightly hypertonic submucosal compartment. The residual inflow cannot be ascribed to residual Na^+ pump activity, as raising the ouabain concentration to 0·5 mM has no significant effect on the residual inflow.

It is possible that there is an ouabain-insensitive component of salt transport. This explanation for residual flux was tested as follows. Raising the D-glucose concentration in the mucosal Ringer solution by 50 mM before addition of ouabain causes only a transient decrease in J_m, as the sugar rapidly crosses the actively transporting tissue and accumulates within the submucosa, thereby reversing the sugar-dependent

osmotic pressure gradient across the mucosa. When, following exposure of the tissue to ouabain for 30 min, D-glucose is raised to 50 mM in the mucosal Ringer solution, the residual water inflow is completely inhibited and does not recover ($n = 3$). This suggests that the residual J_m is not due to an ouabain-insensitive active accumulation of fluid, as in this case recovery of residual inflow would be predicted once glucose equilibration between the mucosa and submucosa had occurred. As the residual mucosal inflow was prevented by raising the tonicity of the mucosal solution, this indicates that it is sustained by a small hypertonicity within the submucosa.

The results of Fig. 3 also indicate that following exposure to ouabain there is a rapid initial increase in outflow across the serosal surface, J_s. There is a simultaneous small increase in mucosal inflow, J_m. This early increase is followed by a decrease in outflow across both the serosal and mucosal surfaces. As the tissue volume is still increasing (J_m exceeds J_s) during the period of inhibition of serosal outflow, the decrease in serosal outflow cannot be ascribed to a volume-dependent decrease in submucosal pressure. It seems that ouabain decreases interstitial pressure, perhaps by reducing the tone of the muscle layers which remain after the serosa and longitudinal muscle layers are removed.

It is clearly necessary to measure the interstitial pressure and distensibility of the submucosa directly. However, even without these pressure measurements, taken together, the independent transient responses of J_m and J_s to hyper- and hypotonicity of the mucosal solution, the presence of heterogeneous pathways for fluid and solute movement across the mucosal surface, the apparent loss of glucose dependence of mucosal inflow after prolonged exposure to 20 mM-D-glucose, the prolonged time required for inhibition of fluid inflow after exposure to high concentrations of ouabain, all indicate a distensible submucosa, containing fluid slightly hypertonic to the mucosal bathing solution, which is an important factor in control of the volume and tonicity of transepithelial and net transmucosal flow.

APPENDIX

A computer model of intestinal water flow based on the experimental findings of this and the previous paper (Naftalin & Tripathi, 1985) has been constructed to aid understanding of the interrelations between the solvent and solute flows.

Water flow. Water is transported across the mucosal surface via three parallel channels (Fig. 1). Net fluid flow across the mucosal surface, J_m (cm s^{-1}) is

$$J_m = J_1 + J_2 + J_3. \quad (1)$$

J_1 is the combined flow between the mucosal solution and lateral intercellular space via the tight-junction and transcellular route, driven by osmotic pressure generated by the salt and solute concentration difference between the mucosal solution, compartment 0 and the lateral intercellular space, compartment 1. The reflexion coefficients of pumped salts and of sucrose of both the transcellular route and tight-junction are close to 1. As the fully engorged lateral intercellular space is assumed to have a fixed volume, inflow J_1 into the lateral intercellular space from the mucosal solution equals outflow from the space into the submucosa.

J_2 is flow across the transcellular route between the mucosal solution and the submucosa, bypassing the lateral intercellular space. The reflexion coefficient of this route towards NaCl and sucrose is also 1. Flow is induced by the osmotic pressure and hydrostatic pressure difference between the mucosal solution, 0 and the submucosal compartment 2. The L_p of the transcellular route, expressed per unit serosal area, is larger than would be predicted on the basis of membrane area exposed to the submucosa alone, because this route includes flows across inactive cells and cells adjacent to spaces with leaky 'tight junctions'.

J_3 is flow via the mucosal shunt pathway between the submucosa and mucosal solution. Flow across this route is driven mainly by interstitial pressure.

J_4, or J_s, is the fluid movement between the submucosal compartment 2 and the serosal reservoir 3. The reflexion coefficient of the serosal surface towards low molecular weight solutes is zero, hence J_4 is driven by hydrostatic pressure from interstitial pressure and the pressure head across a tissue supported at the serosal surface.

Solute flow. F_1 is the solute flow across the tight-junction and transcellular route between mucosal solution lateral intercellular space. Because the reflexion coefficients for NaCl and sucrose are approximately 1, passive solute flow across this route is small. The main source of solute within the lateral intercellular space is NaCl pumped by the action of the Na^+ pump; this pumps at rate J_p (nmol cm^{-2} s^{-1}). The ultimate source of the pumped salt is assumed to arise from the mucosal solution.

F_2 is solute flow between the lateral intercellular spaces and submucosa. The reflexion coefficient at the basal opening of the lateral intercellular space towards all solutes = 0. However, the diffusive barrier between the lateral intercellular space and submucosa is an important determinant of the capacity of the tissue to move water against a transepithelial salt concentration gradient (Weinstein & Stephenson, 1981).

F_3 and F_4 are solute flows between the submucosa and mucosal solution via the mucosal shunt pathway and the serosal fluid conductance channels respectively.

Solvent and solute flows are modelled by the first-order Kedem & Katchalsky equations (1958). The general equation for water flow, J_i (cm^3 cm^{-2} s^{-1}) across any barrier, i is:

$$J_i = -L_i \cdot (2RT \cdot (C_a - C_b) \cdot \sigma_{iC} + RT \cdot (R_a - R_b) \cdot \sigma_{iR} + P_t + P_h). \quad (2)$$

The general equation for F_i is:

$$F_i = P_{iC} \cdot (C_a - C_b) + P_{iR} \cdot (R_a - R_b) + J_i \cdot (1 - \sigma_{iC}) \cdot (C_a + C_b)/2 + J_i \cdot (1 - \sigma_{iR}) \cdot (R_a + R_b)/2 + J_p(C). \quad (3)$$

C_a and C_b, and R_a and R_b are the concentrations (mM) of pumped salt (NaCl) and non-pumped solute (sucrose) in compartments a and b. RT is the product of gas constant and absolute temperature = 26 cmH_2O mM^{-1} at 37 °C. σ_{iR}, σ_{iC} are the reflexion coefficients of R and C at any barrier i (dimensionless). The pressure head, P_h, (cmH_2O) acts across only the barrier resting on an external rigid support, in this case the serosal barrier (Naftalin & Tripathi, 1985). Interstitial pressure, P_t (cmH_2O), acts across both mucosal and serosal barriers. J_p is the pump flux of NaCl into the lateral intercellular space (nmol cm^{-2} s^{-1}). L_i is the hydraulic conductance

(cm s^{-1} cmH_2O^{-1}) across any barrier i. Flows are all expressed per square centimetre of serosal area. P_{iC} and P_{iR} are the permeability coefficients (cm s^{-1}) of barrier i to C and R respectively.

The volume of the submucosa, V_2 (cm^3 cm^{-2}) at any time t, depends on the aggregate of fluid flows across the mucosal and serosal surfaces and on the resting volume, V_0 (cm) over the time interval (t^2–t^1). V_2 is obtained by numerical integration of the flows, J_i.

$$V_2 = V_0 + \int_{t^1}^{t^2} (J_m - J_4)\,dt.$$

The interstitial pressure, P_t (cmH_2O) is obtained from the following relationship:

$$P_t = (V_2 - V_0)/(V_0 . Di),$$

where Di (cmH_2O^{-1}) is the tissue distensibility. Tissue expansion leads to an increase in interstitial pressure. The amounts of solute within the lateral intercellular space, A_1, and submucosal compartments, A_2, are obtained by numerical integration of the solute flow equations. Hence C_1 the osmotic concentration of pumped solute in the lateral intercellular space at any time, is A_1/V_1. The solute concentration, C_2 within the submucosa is A_2/V_2.

A_1, A_2 and V_2, are obtained by simultaneous solution of the differential equations for each of these variables. This is done using fourth-order Runge–Kutta numerical integration procedures. Solutions were obtained using an Apple II 48K microcomputer with a program written in Applesoft Basic.

The L_p values and solute permeabilities and reflexion coefficients used are determined from the experimental procedures described in this and the previous paper (Naftalin & Tripathi, 1985) (see legend to Fig. 9 of this paper). The pump flux J_p is chosen to match the net transepithelial NaCl flow across rabbit ileum in the presence of D-glucose = 0·5–1·5 nmol cm^{-2} s^{-1} (Simmons & Naftalin, 1976). The volume of the lateral intercellular space, V_1, is assumed to be approximately 40 % of the total extracellular volume (i.e. 0·02 cm^3 cm^{-2} serosal area). This value is consistent with electron-microscopic studies of other transporting epithelia (Bindslev, Tormey & Wright, 1974; Blom & Helender, 1977). The initial resting submucosal volume (0·03 cm^3 cm^{-2}) is obtained from the known weights, extracellular space volume measurements (Simmons & Naftalin, 1976; Esposito, Faelli, Tosco, Burlini & Capraro, 1979).

The tissue distensibility, Di (range 1×10^{-3}–5×10^{-4} cmH_2O^{-1}) is chosen to give a pressure rise of 10–50 cmH_2O for a 10 % increase in submucosal volume. These values are consistent with the estimated interstitial pressures and the observed increments in tissue volume (Mortillaro & Taylor, 1976; Naftalin & Tripathi, 1985), but have not been measured directly.

Simulation of osmotic flow transients across rabbit intestine

Hypotonicity. Following a period of 20 min during which the tissue reaches a quasi-stable absorption, the tonicity of the mucosal bathing solution is reduced by 50 mosmol kg^{-1} (half-time for mixing 13·5 s). Fig. 9*A* shows the simulated changes in net water flows, J_m and J_s. Inflow across the mucosal surface, J_m, rises from 10

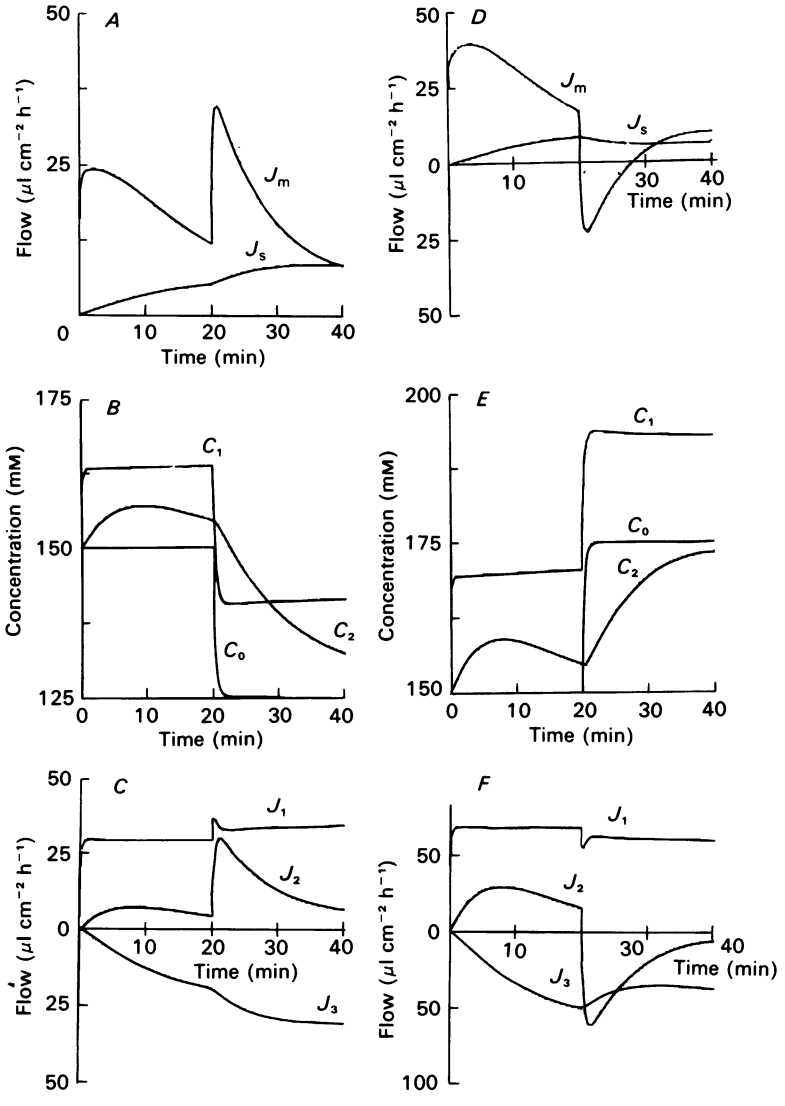

Fig. 9. *A*, *B*, *C*, simulation of the effects of 50 osmol kg^{-1} hypotonicity in the mucosal solution, initial tonicity 300 mosmol kg^{-1} (half-time for mixing = 13·86 s), after 20 min absorption, on: *A*, J_m and J_s; *B*, C_0 (mucosal concentration), C_1 (lateral intercellular space concentration) and C_2 (submucosal concentration of NaCl); *C*, mucosal flows J_1, J_2 and J_3. *D*, *E*, *F*, simulation of the effect of 50 mosmol kg^{-1} hypertonicity (NaCl) in the mucosal solution (half-time of mixing = 13·68 s) after 20 min absorption; on: *D*, J_m and J_s; *E*, C_0 (mucosal solution tonicity); C_1 (lateral intercellular space tonicity), C_2 (submucosal compartment tonicity); *F*, mucosal flows J_1, J_2 and J_3.

Model parameters: $L_1 = 1 \times 10^{-8}$; $L_2 = 9 \times 10^{-9}$; $L_3 = 1{\cdot}5 \times 10^{-7}$; $L_4 = 5 \times 10^{-8}$ cm s^{-1} cmH_2O^{-1}; $Di = 6 \times 10^{-3}$ cmH_2O^{-1}; $J_p = 1{\cdot}5$ nmol s^{-1}; $P_1 = 1 \times 10^{-7}$; $P_2 = 1 \times 10^{-6}$; $P_3 = 7 \times 10^{-5}$; $P_4 = 2 \times 10^{-5}$ cm s^{-1}. Reflexion coefficients of NaCl at tight junction 0·95, mucosal shunt 0. Lateral intercellular space volume, $V_1 = 25$ μl cm^{-2}; initial submucosal volume, $V_2 = 30$ μl cm^{-2}.

to 35 μl cm^{-2} h^{-1} within 30 s and then steadily declines to 10 μl cm^{-2} h^{-1} during the next 10 min period. There is a small rise in J_s from 5 to 10 μl cm^{-2} h^{-1}. Fig. 5 shows similar changes in J_m and J_s after dilution of the mucosal solution.

The simulated changes in salt concentration within the lateral intercellular space C_1 and submucosal space C_2 are shown in Fig. 9*B*; C_0 shows the perturbation in mucosal solution tonicity. Because the lateral intercellular space is small (20 μl cm^{-2}) and inelastic, and the mucosal L_p substantial ($L_1 \approx 1 \times 10^{-8}$ cm s^{-1} cmH_2O^{-1}), the solute concentration within the lateral intercellular space, C_1, falls within a few seconds to a new steady state. However, the decrease in submucosal tonicity, C_2, is much slower, since the submucosal volume is large and distensible, solute exit from the submucosa is only slightly affected by convective flows, and also solute diffusion via the mucosal shunt and serosal pathways is slow (half-time for equilibration 7–10 min).

Fig. 9*C* shows the resolved flows J_1, J_2 and J_3. Following dilution of the mucosal solution, there is a small transient increase in J_1, as C_1 rapidly falls to its new steady state. However, there is substantial increase in J_2, the transcellular flow, because the osmotic pressure gradient between the submucosa and mucosal solution is slow to dissipate. J_3, the flow via the musocal shunt, increases as tissue volume and hence, interstitial pressure, rises.

Hypertonicity. Simulation of the effect of increasing the tonicity of the mucosal solution by 50 mosmol NaCl kg^{-1} (half-time of mucosal solution mixing = 13·8 s), on J_m and J_s is shown in Fig. 9*D*. Following osmotic perturbation, there is a rapid reversal of J_m. J_m then recovers within 7 min to positive net inflow. During this period J_s falls slightly. These effects are as observed (see Fig. 6). Following the rise in mucosal solution tonicity, C_0, from 150 to 175 mM, the solute concentration within the lateral intercellular space, C_1, rises rapidly (seconds) to a new steady state. The submucosal concentration, C_2, rises slowly as solute diffuses in via the shunt pathway and water is lost via the transcellular route (Fig. 9*E*). The resolved mucosal flows J_1, J_2 and J_3 are shown in Fig. 9*F*. Because C_1 equilibrates rapidly there is only a small and rapid perturbation in J_1, which is muffled by the unstirred layer effect at the external mucosal surface. However, J_2, the transcellular flow, is large and sustained, as the osmotic pressure gradient between the submucosa and mucosal solution equilibrates slowly. As during this phase the tissue loses volume, the interstitial pressure falls, and hence outflows via both the mucosal shunt pathway J_3 and via the serosal surface J_s (Fig. 9*D*) decrease.

Following either hyper-, or hypotonic perturbation, this model predicts that the solute concentration within the lateral intercellular space remains 40–50 mosmol kg^{-1} above that of the mucosal solution, whereas the submucosal tonicity approaches the mucosal solution within 10–20 min.

The authors wish to thank the M.R.C. for financial support. The assistance of Drs P. Smith and M. Ahsan and Mr Bob Roberts is gratefully acknowledged. Copies of the Basic computer program listing for simulation of quasi-isotonic flows are available. Disk copies can be made available to run on Apple DOS 3·3.

REFERENCES

BARRY, P. H. & DIAMOND, J. M. (1984). Effects of unstirred layers on membrane phenomena. *Physiological Reviews* **64**, 763–872.

BINDSLEY, N., TORMEY, J. McD. & WRIGHT, E. M. (1974). The effects of electrical and osmotic gradients on lateral intercellular spaces and membrane conductance in a low resistance epithelium. *Journal of Membrane Biology* **19**, 357–380.

BLOM, H. & HELENDER, H. F. (1977). Quantitative electron microscopical studies on *in vitro* incubated rabbit gallbladder epithelium. *Journal of Membrane Biology* **37**, 45–61.

CRANE, R. K. (1977). The gradient hypothesis and other models of carrier-mediated active transport. *Reviews of Physiology, Biochemistry and Pharmacology* **78**, 101–158.

CURRAN, P. F. (1960). Na, Cl and water transport by rat ileum *in vitro*. *Journal of General Physiology* **43**, 1137–1148.

CURRAN, P. F. & McINTOSH, J. R. (1962). A model for biological water transport. *Nature* **193**, 347–348.

DIAMOND, J. M. (1966). A rapid method for determining voltage–concentration relations across membranes. *Journal of Physiology* **183**, 83–100

DIAMOND, J. M. (1979). Osmotic water flow in leaky epithelia. *Journal of Membrane Biology* **51**, 195–216.

DIAMOND, J. M. & BOSSERT, W. H. (1967). Standing gradient osmotic water flow: a mechanism for coupling of water and solute transport in epithelia. *Journal of General Physiology* **50**, 2061–2083.

DURBIN, R. P. (1960). Osmotic flows of water across permeable cellulose membranes. *Journal of General Physiology* **44**, 315–326.

ESPOSITO, G., FAELLI, A., TOSCO, M., BURLINI, N. & CAPRARO, V. (1979). Extracellular space determination of rat small intestine by using markers of different molecular weight. *Pflügers Archiv* **382**, 67–71.

GUPTA, B., HALL, T. A. & NAFTALIN, R. J. (1978). Microprobe measurement of Na, K and Cl concentration profiles in epithelial cells and intercellular spaces. *Nature* **272**, 70–73.

HILL, A. E. (1975). Solute–solvent coupling in epithelia: a critical examination of the standing-gradient osmotic flow theory. *Proceedings of the Royal Society* B **190**, 99–114.

HILL, A. E. (1980). Salt–water coupling in leaky epithelia. *Journal of Membrane Biology* **56**, 177–182.

KEDEM, O. & KATCHALSKY, A. (1958). Thermodynamic analysis of the permeability of biological membranes to non electrolytes. *Biochimica et biophysica acta* **27**, 229–246.

MORTILLARO, N. A. & TAYLOR, A. E. (1976). Interaction of capillary and tissue forces in cat small intestine. *Circulation Research* **36**, 348–358.

NAFTALIN, R. J. & TRIPATHI, S. (1982*a*). A high-resolution method for continuous measurement of transepithelial water movements across isolated sheets of rabbit ileum. *Journal of Physiology* **326**, 3–4*P*.

NAFTALIN, R. J. & TRIPATHI, S. (1982*b*). Determination of the hydraulic conductivities of the mucosal and serosal surfaces of the isolated rabbit ileum. *Journal of Physiology* **329**, 69*P*.

NAFTALIN, R. J. & TRIPATHI, S. (1982*c*). The effects of changing tonicity of the mucosal solution on fluid transport by isolated rabbit ileum. *Journal of Physiology* **332**, 112–113.

NAFTALIN, R. J. & TRIPATHI, S. (1983). Routes of water flow across the intestine and their relationship to isotonic flow. In *Intestinal Transport*, ed. GILLES BAILLIEN, M. & GILLES, R., pp. 14–25. Berlin, Heidelberg: Springer-Verlag.

NAFTALIN, R. J. & TRIPATHI, S. (1985). Passive water flows driven across the isolated rabbit ileum by osmotic, hydrostatic and electrical gradients. *Journal of Physiology* **360**, 27–50.

PARSONS, D. S. & WINGATE, D. L. (1961). The effects of osmotic gradients on fluid transfer across rat intestine *in vitro*. *Biochimica et biophysica acta* **46**, 170–183.

RENKIN, E. & GILMORE, J. E. (1973). *Handbook of Physiology, Renal Physiology*, ed. ORLOFF, J. & BERLINER, R. W., pp. 185–248. Baltimore: American Physiological Society, Williams & Wilkins.

SACKIN, H. & BOULPAEP, E. (1975). Models for coupling of salt and water transport. Proximal tubular reabsorption in *Necturus* kidney. *Journal of General Physiology* **66**, 671–733.

SCHULTZ, S. G. & SOLOMON, A. K. (1961). Determination of the effective hydrodynamic radii of small molecules by viscometry. *Journal of General Physiology* **44**, 1189–1199.

SIMMONS, N. L. & NAFTALIN, R. J. (1976). Factors affecting the compartmentalization of sodium ion within rabbit ileum *in vitro*. *Biochimica et biophysica acta* **448**, 411–425.

SMYTH, H. & TAYLOR, C. B. (1957). Coupled transport of water and solutes by an *in vitro* intestinal preparation. *Journal of Physiology* **136**, 632–648.

VAN HEESWIJK, M. P. E. & VAN OS, C. H. (1984). Hydraulic conductivity of rabbit brush-border membrane vesicles. *Journal of Physiology* **348**, 27*P*.

WEINSTEIN, A. M. & STEPHENSON, J. L. (1981). Model of coupled salt and water transport across leaky epithelia. *Journal of Membrane Biology* **60**, 1–20.

WRIGHT, E. M., SMULDERS, A. P. & TORMEY, J. McD. (1972). The role of the lateral intercellular spaces and solute polarization effects in the passive flow of water across the rabbit gallbladder. *Journal of Membrane Biology* **7**, 198–219.